Journal of Thermal Analysis and Calorimetry, Vol. 95 (2009) 1, 123–129

THERMAL DECOMPOSITION OF HYDROTALCITES WITH VARIABLE CATIONIC RATIOS

Sara J. Palmer, H. J. Spratt and R. L. Frost[*]

Inorganic Materials Research Program, School of Physical and Chemical Sciences, Queensland University of Technology
GPO Box 2434, Brisbane Queensland 4001, Australia

Thermal analysis complimented with evolved gas mass spectrometry has been applied to hydrotalcites containing carbonate prepared by coprecipitation and with varying divalent/trivalent cation ratios. The resulting materials were characterised by XRD, and TG/DTG to determine the stability of the hydrotalcites synthesised. Hydrotalcites of formula $Mg_4(Fe,Al)_2(OH)_{12}(CO_3)\cdot 4H_2O$, $Mg_6(Fe,Al)_2(OH)_{16}(CO_3)\cdot 5H_2O$, and $Mg_8(Fe,Al)_2(OH)_{20}(CO_3)\cdot 8H_2O$ were formed by intercalation with the carbonate anion as a function of the divalent/trivalent cationic ratio.

XRD showed slight variations in the d-spacing between the hydrotalcites. The thermal decomposition of carbonate hydrotalcites consists of two decomposition steps between 300 and 400°C, attributed to the simultaneous dehydroxylation and decarbonation of the hydrotalcite lattice. Water loss ascribed to dehydroxylation occurs in two decomposition steps, where the first step is due to the partial dehydroxylation of the lattice, while the second step is due to the loss of water interacting with the interlayer anions. Dehydroxylation results in the collapse of the hydrotalcite structure to that of its corresponding metal oxides and spinels, including MgO, $MgAl_2O_4$, and $MgFeAlO_4$.

Keywords: *carbonate, hydrotalcite, pyroaurite, thermal analysis, X-ray diffraction*

Introduction

Hydrotalcites, or layered double hydroxides (LDH's) are fundamentally anionic clays, and are less well-known than cationic clays like smectites [1, 2]. The structure of hydrotalcite can be derived from a brucite structure ($Mg(OH)_2$) in which e.g. Al^{3+} or Fe^{3+} (pyroaurite-sjögrenite) substitutes a part of the Mg^{2+} [3–14]. This substitution creates a positive layer charge on the hydroxide layers, which is compensated by interlayer anions or anionic complexes [15, 16]. When LDHs are synthesised any appropriate anion can be placed in the interlayer. These anions may be any anion with a suitable negative charge including the phosphate anion. The hydrotalcite may be considered as a gigantic cation which is counterbalanced by anions in the interlayer. In hydrotalcites a broad range of compositions are possible of the type $[M^{2+}_{1-x}M^{3+}_{x}(OH)_2]^{x+}[A^{n-}]_{x/n}\cdot yH_2O$, where M^{2+} and M^{3+} are the di- and trivalent cations in the octahedral positions within the hydroxide layers with x normally between 0.17 and 0.33. It is normal practice to determine the composition of the formed hydrotalcite by chemical means such as ICP-AES or EDAX techniques. A^{n-} is an exchangeable interlayer anion [17–19]. In the hydrotalcites reevesite and pyroaurite, the divalent cations are Ni^{2+} and Mg^{2+} respectively with the trivalent cation being Fe^{3+}. In these cases, the carbonate anion is the major interlayer counter anion.

Thermal analysis using thermogravimetric techniques enables the mass loss steps, the temperature of the mass loss steps and the mechanism for the mass loss to be determined [6, 11, 20–24]. Thermoanalytical methods provide a measure of the thermal stability of the hydrotalcite. The reason for the potential application of hydrotalcites as catalysts rests with the ability to make mixed metal oxides at the atomic level, rather than at a particle level. Such mixed metal oxides are formed through the thermal decomposition of the hydrotalcite [25, 26]. There are many other important uses of hydrotalcites such as in the removal of environmental hazards in acid mine drainage [27, 28], and a mechanism for the disposal of radioactive wastes [29]. Their ability to exchange anions presents a system for heavy metal removal from contaminated waters [30]. Structural information on different minerals has successfully been obtained recently by sophisticated thermal analysis techniques [6, 20–24].

The decomposition of the Mg, Al hydrotalcite structure occurs in three steps:

- removal of adsorbed water (<100°C),
- elimination of the interlayer structural water (100–200°C), and

* Author for correspondence: r.frost@qut.edu.au

1388–6150/$20.00

Akadémiai Kiadó, Budapest, Hungary
Springer, Dordrecht, The Netherlands

- the simultaneous dehydroxylation and decarbonation of the hydrotalcite framework (300–400°C) [6, 31–38].

A fourth decomposition step may occur for the loss of either a volatile anion species (e.g. Cl^-, NO_3^-, and CO_3^{2-}) or a non-volatile species in which the anion is included in the formation of a mixed metal oxide [31, 35, 38]. The determination of the decomposition steps of hydrotalcite depends on the dryness of the sample, stability of the interlamellar species, and possible guest-host interactions mobilising the hydroxyl groups in the hydrotalcite lattice [35]. Dehydroxylation results in the collapse of the hydrotalcite structure to that of its corresponding metal oxides, including MgO, Al_2O_3, and $MgFeAlO_4$ (at temperatures over 900°C) [6, 33]. The exact decomposition product relies on the hydrotalcite and its counter balancing anions.

Thermal analysis has proven most useful for the study of the thermal stability of hydrotalcites [11, 39–42]. In this work we report the thermal analysis of hydrotalcite with carbonate in the interlayer and explore the effect of the divalent/trivalent ratio on hydrotalcite formation. The objective of this research is to determine the thermal stability of hydrotalcites synthesised with different divalent/trivalent cationic ratio.

Experimental

Preparation of mixed metal ion solution

Varying amounts of aluminium chloride hexahydrate, iron(III) chloride hexahydrate and magnesium chloride hexahydrate were dissolved in 500 mL of ultra pure water. The ratio of moles of M^{2+} to M^{3+}, where *M* is a metal, in the different solutions was: 2:1, 3:1 and 4:1. The following table summarises the quantity of each metal dissolved in 500 mL of water.

Table 1 Quantity of each metal dissolved in 500mL of water

	2:1 solution	3:1 solution	4:1 solution
Magnesium	67.765 g	76.240 g	81.320 g
Aluminium	11.110 g	8.335 g	6.665 g
Iron(III)	22.525 g	16.895 g	13.515 g

The chosen metal ion solution was then added drop wise into the caustic solution (2 M NaOH and 0.2 M Na_2CO_3) via a peristaltic pump. The solution was then vacuum filtered, washed thoroughly with hot degassed water and dried in an oven overnight at 120°C.

Methods

X-ray diffraction

X-ray diffraction patterns were collected using a Philips X'pert wide angle X-ray diffractometer, operating in step scan mode, with CuK_α radiation (1.54052 Å). Patterns were collected in the range 3 to 90° 2θ with a step size of 0.02° and a rate of 30 s per step. Samples were prepared as a finely pressed powder into aluminium sample holders. The Profile Fitting option of the software uses a model that employs twelve intrinsic parameters to describe the profile, the instrumental aberration and wavelength dependent contributions to the profile.

Thermal analysis

Thermal decomposition of the hydrotalcite was carried out in a TA® Instruments incorporated with a high-resolution thermogravimetric analyser (series Q500) in a flowing nitrogen atmosphere (80 cm^3 min^{-1}). Approximately 50 mg of sample was heated in an open platinum crucible at a rate of 5.0°C min^{-1} up to 1000°C at high resolution. The TG instrument was coupled to a Balzers (Pfeiffer) mass spectrometer for gas analysis. Only selected gases such as water and carbon dioxide were analysed.

Results and discussion

X-ray diffraction

The X-ray diffraction patterns for the carbonate interlayer hydrotalcites are shown in Fig. 1a. The XRD patterns of the decomposition products of the 2:1, 3:1 and 4:1 hydrotalcites are given in Figs 1b–d, respectively. Hydrotalcite normally has a $d_{(003)}$ spacing of around 7.9 Å [43, 44]. The XRD patterns show that the *d*-spacing for the carbonate interlayer

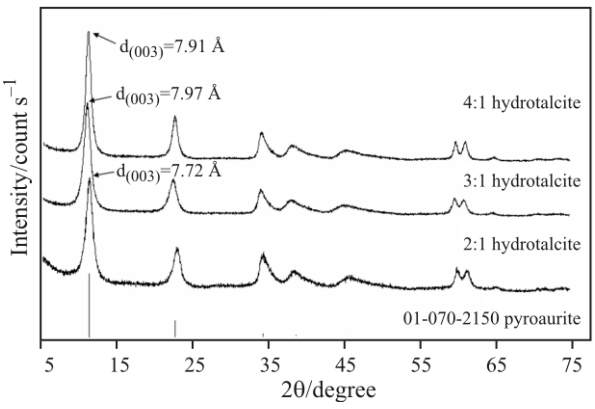

Fig. 1a XRD patterns and references for the synthesised hydrotalcites with varying cationic ratios

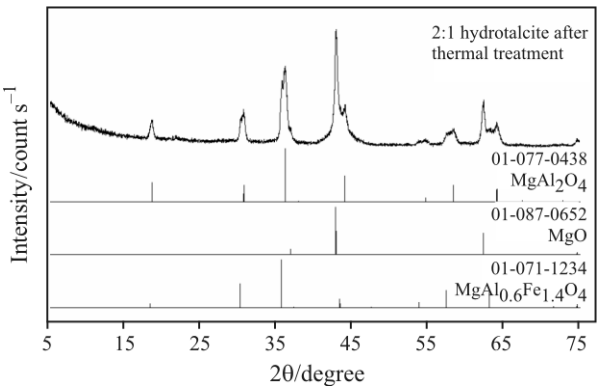

Fig 1b XRD patterns of the synthesized 2:1 hydrotalcite after thermal analysis treatment

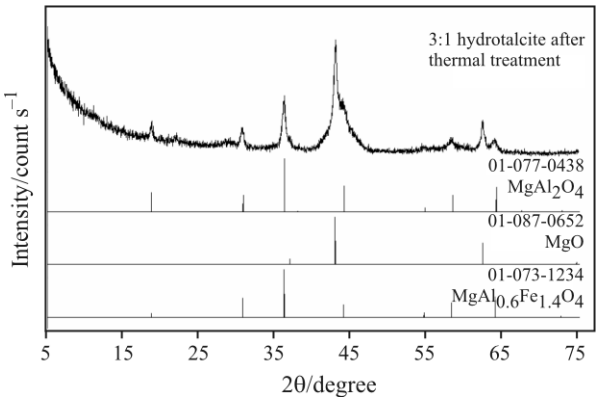

Fig 1c XRD patterns of the synthesized 3:1 hydrotalcite after thermal analysis treatment

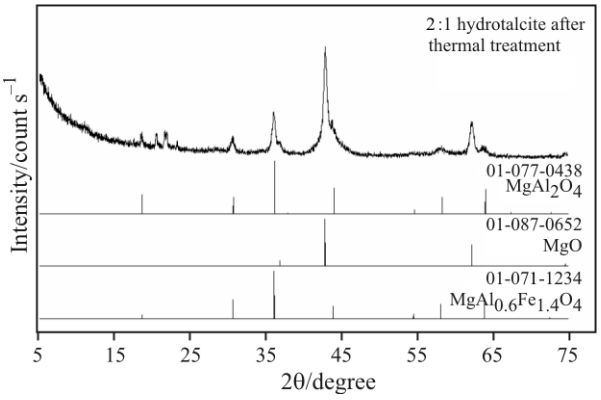

Fig. 1d XRD patterns of the synthesized 4:1 hydrotalcite after thermal analysis treatment

hydrotalcite is cation dependent. The XRD patterns obtained for the synthetic hydrotalcites match closely with reference pattern 01-070-2150 (pyroaurite – $Fe_2Mg_6(OH)_{16}CO_3(H_2O)_{4.5}$). The method of synthesis for these hydrotalcites allows for the possibility of a variety of products including: hydrotalcite, pyroaurite and other forms of hydrotalcites with a mixture of cationic ratios. However, there appears to be only one phase present in the XRD pattern, suggesting that multiple phases were not produced. Minor quantities may have been produced but were not detected using XRD. The $d_{(003)}$ obtained for the synthesised hydrotalcites were 7.72, 7.97 and 7.91 Å, 2:1, 3:1 and 4:1 hydrotalcite respectively. The increase in *d* spacing for the 3:1 and 4:1 hydrotalcites indicates an increase in the interlayer region of these hydrotalcites.

Thermogravimetry

The dehydroxylation step for hydrotalcite is generally observed at around 300°C [6, 31–38]. The results obtained in this investigation agree with literature, with dehydroxylation occurring at 322, 324 and 312°C for the 2:1, 3:1, and 4:1 hydrotalcites respectively. The point of dehydroxylation can be used as an indication of the thermal stability of the hydrotalcite, where a delay in dehydroxylation (higher temperature) indicates increased thermal stability. In regards to the hydrotalcites synthesised it is observed that the 3:1 hydrotalcites are more stable than the 2:1 and 4:1 hydrotalcites, with the 4:1 hydrotalcite having the lowest stability. This decrease in stability of the 4:1 hydrotalcite is believed to be attributed to the increased positive charge of the brucite-like layers, which would require a larger number of anions to counter-balance the charge. The DTG curve for the 2:1 hydrotalcite distinctly shows 2 mass loss steps, corresponding to first dehydroxylation and then decarbonation. However, for the 3:1 and 4:1 hydrotalcites only a single mass loss step is observed indicating that dehydroxylation and decarbonation occur simultaneously. The ion current curves for the three hydrotalcites show that water vapour and CO_2 evolve at these temperatures. The mass spectrometer detected chloride gases (m/Z=35 and 32) in all three of the hydrotalcites synthesised, figures not shown. This suggests that chloride was intercalated into the hydrotalcites along with carbonate, however carbonate was the more dominant anion.

2:1 Metal ion solution

The thermogravimetric and differential thermogravimetric analysis of the 2:1 hydrotalcite of proposed formula $Mg_4(Fe,Al)_2(OH)_{12}(CO_3)\cdot 4H_2O$ is shown in Fig. 2a. The ion current curves for selected evolved gases are shown in Fig. 2b. The ion current curves for the 3:1 and 4:1 hydrotalcite are almost identical to the 2:1 hydrotalcite. Therefore, only the 2:1 ion current curves are given. A very small mass loss step between 25 and 42°C of 0.76% is observed and attributed to the loss of physiosorbed water. Over the temperature range 42 and 200°C, a mass loss of 14.42% is observed and attributed to the loss of both

adsorbed and interlayer water of the hydrotalcite structure. The theoretical mass loss of adsorbed water for the 2:1 hydrotalcite is 13.96%, which is in good agreement with the experimental mass loss. The *m*/*Z*=17 and 18 ion current curves display a broad peak over this temperature range, indicating the removal of the remaining adsorbed water on the hydrotalcite surface. The following thermal decomposition is proposed:

$$Mg_4(Al,Fe)_2(OH)_{12}(CO_3)\cdot xH_2O \rightarrow Mg_4(Al,Fe)_2(OH)_{12}(CO_3)+xH_2O$$

The number of moles of water for this hydrotalcite is 4, shown in the appendix. Therefore, four H_2O molecules are either absorbed or intercalated into this hydrotalcite structure. Two mass loss steps are observed at 322 and 338°C with a total mass loss of 24.48%. The ion current curves for *m*/*Z*=17 and 18 show two maxima at around 325 and 340°C attributed to evolved water vapour at these temperatures confirming the loss of OH units at these temperatures. The ion current curves for *m*/*Z*=44 and 12 show maxima at ~350°C confirming the evolution of CO_2 at this temperature as well, attributed to the thermal decomposition of the carbonate anion. The DTG curve shows the separation of these decomposition steps (shoulder at 338°C), the first due to the partial dehydroxylation of the lattice followed by the simultaneous dehydroxylation and decarbonation of the hydrotalcite structure. A small shoulder at approximately 400°C is due to the further loss of CO_3^{2-} in the form of CO_2, as shown in Fig. 2b. This peak is present in the three hydrotalcites synthesised and is believed to be due to the formation of an intermediate species during the decarbonation of the hydrotalcite structure, such as $Fe_2(CO_3)_3$.

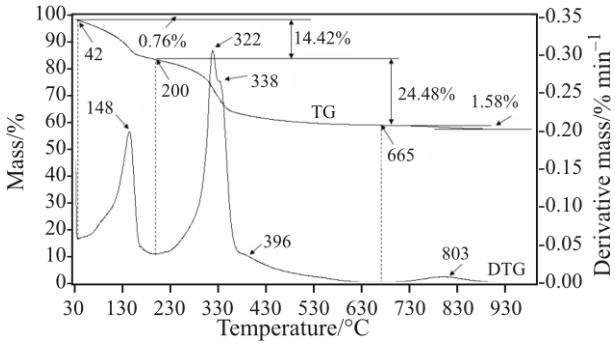

Fig. 2a TG/DTG of the synthesised 2:1 hydrotalcite

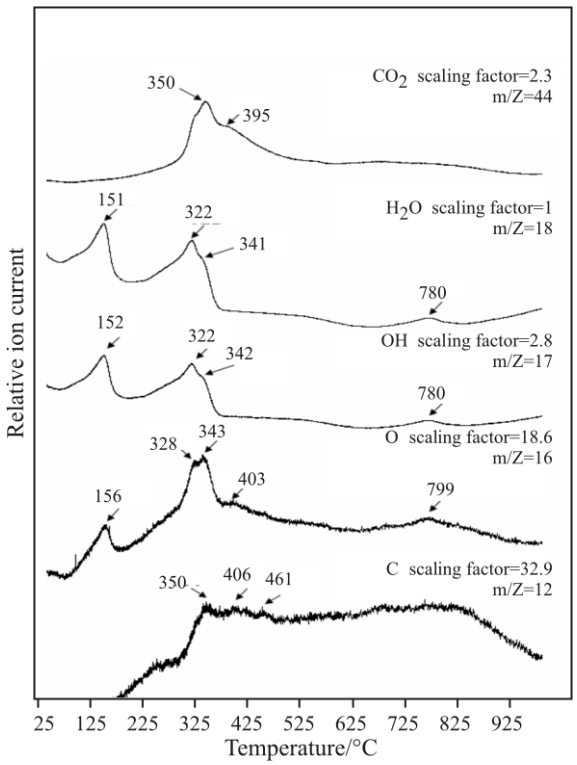

Fig. 2b Ion current curves of evolved gases for the synthesised 2:1 hydrotalcite

The following reaction is proposed for the dehydroxylation and decarbonation of the structure to its corresponding oxides:

$$2Mg_4(Al,Fe)_2(OH)_{12}(CO_3) \rightarrow MgAl_2O_4+6MgO+MgFeAlO_4+2CO_2+12H_2O$$

The decomposition products proposed were confirmed by XRD analysis (Fig. 1b). The molecular mass of this compound is on average 444 molecular mass units, based on a hydrotalcite structure with both Al^{3+} and Fe^{3+} in the structure. The theoretical mass loss associated with the evolution of water vapour and CO_2 is 24.34 and 9.91%, respectively. The experimental mass loss between 200–665°C is 24.48%. A higher temperature mass loss at around 803°C of 1.58% is observed and is believed to be due to the loss of HCl from residual salt present in the precipitate.

3:1 Metal ion solution

The thermogravimetric analysis of the 3:1 hydrotalcite of proposed formula $Mg_6(Fe,Al)_2(OH)_{16}(CO_3)\cdot 5H_2O$ is shown in Fig. 3. The number of water molecules is determined using the percentage mass loss between 0–200°C, which corresponds to the adsorbed and intercalated water in the hydrotalcite structure, calculations are given in the appendix. The molecular mass of this compound is approximately 651 molecular mass units, dependent on which cation is substituted into the brucite-like layer. The mass loss over the temperature range 25 to 65°C is 0.58% attributed to the loss of adsorbed water. The ion current curves for *m*/*Z*=17 and 18, figure not shown, prove water is the evolved gas at this temperature range. A further mass loss of

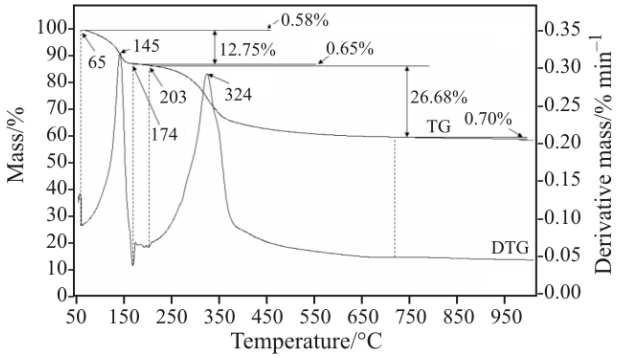

Fig. 3 TG/DTG of the synthesised 3:1 hydrotalcite

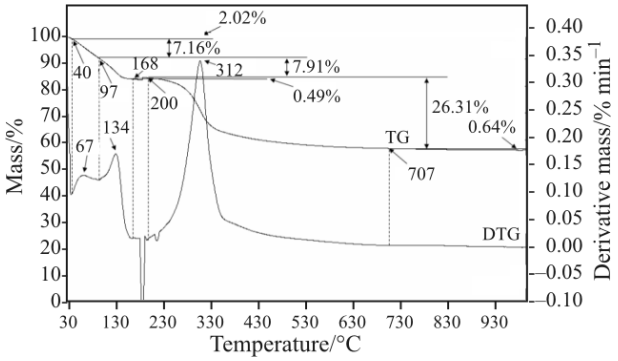

Fig. 4 TG/DTG of the synthesised 4:1 hydrotalcite

12.75% at 145°C is observed. The theoretical mass loss of adsorbed and intercalated water is 13.84%, which is in good agreement with the experimental results obtained. Again the ion current curves indicate that water vapour is evolved at these temperatures. These mass losses are attributed to the loss of water from the interlayer of the hydrotalcite. A broad mass loss step is observed at 324°C with a total mass loss of 26.68%. The ion current curves for m/Z=17 and 18 show a broad maxima at around 311°C with a shoulder present at 354°C attributed to evolved water vapour, confirming the loss of OH units at these temperatures. The ion current curves for m/Z=44 and 12, figure not shown, also shows a maxima at ~350°C confirming the evolution of CO_2 at this temperature. This peak is not as defined as the corresponding peak in the 2:1 hydrotalcite, due to a smaller ratio of CO_3^{2-} being expected in the 3:1 hydrotalcite compared to the number of OH units in the hydrotalcite structure. The evolution of gases attributed to both OH and carbonate units suggests the simultaneous dehydroxylation and decarbonation of the hydrotalcite structure occurs in the same temperature range. The following reaction is proposed:

$$2Mg_6(Al,Fe)_2(OH)_{16}(CO_3)\rightarrow MgAl_2O_4+MgFeAlO_4+10MgO+2CO_2+16H_2O$$

The decomposition products proposed were confirmed by XRD analysis (Fig. 1c). The theoretical mass losses according to this formula of CO_2 and OH units are 7.85 and 25.70%, respectively.

4:1 Metal ion solution

The thermogravimetric and differential thermogravimetric curves for the thermal decomposition of the 4:1 hydrotalcite is shown in Fig. 4. The proposed formula for the 4:1 hydrotalcite is $Mg_8(Fe,Al)_2(OH)_{20}(CO_3)\cdot 8H_2O$. The number moles of water are calculated using the method shown in the appendix. Thus the molecular mass is between 820 amu, dependent on the cationic composition of the hydrotalcite. The theoretical mass loss due to adsorbed water and intercalated water is 17.58%. Mass loss steps of 2.02 and 7.16% at low temperatures is observed up to around 65°C, and is attributed to the removal of water adsorbed on the surface. A further mass loss step of 7.91% at 135°C is attributed to the dehydration of the hydrotalcite interlayer. A total mass loss of 17.09% is observed and is in good agreement with the expected mass loss. The ion current curves prove the evolution of water vapour at the corresponding temperatures.

A single mass loss of 26.31% is found at 312°C. The ion current curves of m/Z=44, 18, 17 and 12, figures not shown, prove that water and CO_2 are the evolved gases at this temperature. This water vapour results from the dehydroxylation of the hydrotalcite. There appears to be a shoulder at 400°C, which is again due to the evolution of CO_2, due to the formation of carbonate species after the decarbonation of the hydrotalcite structure. The shape of the DTG curve also looks more symmetrical, and this is believed to be due to the smaller quantity of carbonate anions in the structure compared to OH units, which influence the shape of the DTG curve more strongly. The evolution of gases attributed to both OH and carbonate units suggests the simultaneous dehydroxylation and decarbonation of the hydrotalcite structure occurs at around 350°C. The following reaction is proposed for the dehydroxylation and decarbonation of the hydrotalcite:

$$2Mg_8(Al,Fe)_2(OH)_{20}(CO_3)\rightarrow MgAl_2O_4+MgFeAlO_4+14MgO+2CO_2+20H_2O$$

The decomposition products proposed were confirmed by XRD analysis (Fig. 1d). The theoretical mass loss of OH units in the dehydrated hydrotalcite structure is 26.60%. The experimental mass loss between 200–700°C is 26.68%.

Conclusions

The decomposition of the synthesised hydrotalcites occurred in 3 steps (1) evaporation of adsorbed water (up to 100°C), (2) elimination of the interlayer structural water (up to 200°C) and (3) dehydroxylation and decarbonation of the hydrotalcite framework (up to 400°C). The ion current curves revealed that dehydroxylation and decarbonation occurred simultaneously. Changes in the shape of the DTG curve were observed, where an increase in divalent/trivalent ratio increase the symmetry of the dehydroxylation/ decarbonation peak, ~350°C. This is believed to be due to the decrease in the ratio of carbonate units, compared to OH units, as the divalent/trivalent ratio increases. The larger number of OH units in the 4:1 hydrotalcite causes the peak corresponding to the decarbonation of the hydrotalcite to be almost insignificant. Dehydroxylation indicates the thermal stability of the hydrotalcite structure, where delays in dehydroxylation indicate a more stable hydrotalcite. Therefore, the order of stability for the synthesised hydrotalcites is 3:1, 2:1 and 4:1 divalent/trivalent cationic ratio. The collapse of the hydrotalcite structure produced corresponding metal oxides, including MgO, $MgAl_2O_4$, and $MgFeAlO_4$.

Acknowledgements

The financial and infra-structure support of the Queensland Research and Development Centre (QRDC-Alcan) and the Queensland University of Technology Inorganic Materials Research Program of the School of Physical and Chemical Sciences is gratefully acknowledged. One of the authors (SJP) is grateful to Alcan for a Masters scholarship. The Australian Research Council (ARC) is thanked for funding the Thermal Analysis Facility.

Appendix

Calculation of water content for $Mg_4(Fe,Al)_2(OH)_{12}(CO_3)\cdot xH_2O$

Composition: $Mg_4(Fe,Al)_2(OH)_{12}(CO_3)\cdot xH_2O$

Removing water up to 200°C: 7.18 mg that is 0.398 mmol of H_2O removed

Remaining dehydrated mineral up to 200°C: 47.27 mg that is 0.0903 mmol

Molar mass of dehydrated mineral: 444.2 g mol^{-1}

Calculation of x:

1 mol dehydrated mineral: x mol H_2O

0.0903 mol dehydrated mineral: 0.398 mol H_2O

x~4 mol

Calculation of water content for $Mg_6(Fe,Al)_2(OH)_{16}(CO_3)\cdot xH_2O$

Composition: $Mg_6(Fe,Al)_2(OH)_{16}(CO_3)\cdot xH_2O$

Removing water up to 203°C: 7.61 mg that is 0.422 mmol of H_2O removed

Remaining dehydrated mineral up to 200°C: 46.83 mg that is 0.084 mmol

Molar mass of dehydrated mineral: 560.9 g mol^{-1}

Calculation of x:

1 mol dehydrated mineral: x mol H_2O

0.084 mol dehydrated mineral : 0.422 mol H_2O

x~5 mol

Calculation of water content for $Mg_6(Fe,Al)_2(OH)_{16}(CO_3)\cdot xH_2O$

Composition: $Mg_8(Fe,Al)_2(OH)_{20}(CO_3)\cdot xH_2O$

Removing water up to 203°C: 7.92 mg that is 0.440 mmol of H_2O removed

Remaining dehydrated mineral up to 200°C: 37.14 mg that is 0.054 mmol

Molar mass of dehydrated mineral: 677.52 g mol^{-1}

Calculation of x:

1 mol dehydrated mineral: x mol H_2O

0.054 mol dehydrated mineral : 0.440 mol H_2O

x~8 mol

References

1 K. Hashi, S. Kikkawa and M. Koizumi, Clays Clay Miner., 31 (1983) 152.
2 L. Ingram and H. F. W. Taylor, Mineral. Magazine J. Miner. Soc., (1876–1968) 36 (1967) 465.
3 J. T. Kloprogge, L. Hickey and R. L. Frost, Mater. Chem. Phys., 89 (2005) 99.
4 R. L. Frost and K. L. Erickson, Spectrochim. Acta, Part A, 61 (2005) 51.
5 K. L. Erickson, T. E. Bostrom and R. L. Frost, Mater. Lett., 59 (2004) 226.
6 R. L. Frost and K. L. Erickson, J. Therm. Anal. Cal., 76 (2004) 217.
7 R. L. Frost and K. L. Erickson, Thermochim. Acta, 421 (2004) 51.
8 J. T. Kloprogge, L. Hickey and R. L. Frost, J. Raman Spectrosc., 35 (2004) 967.
9 J. T. Kloprogge, L. Hickey and R. L. Frost, J. Solid State Chem., 177 (2004) 4047.
10 R. L. Frost and Z. Ding, Thermochim. Acta, 405 (2003) 207.
11 R. L. Frost, W. Martens, Z. Ding and J. T. Kloprogge, J. Therm. Anal. Cal., 71 (2003) 429.
12 R. L. Frost, M. L. Weier, M. E. Clissold and P. A. Williams, Spectrochim. Acta, Part A, 59 (2003) 3313.
13 R. L. Frost, M. L. Weier, M. E. Clissold, P. A. Williams and J. T. Kloprogge, Thermochim. Acta, 407 (2003) 1.

14 R. L. Frost, M. L. Weier and J. T. Kloprogge, J. Raman Spectrosc., 34 (2003) 760.
15 R. M. Taylor, Clay Miner., 17 (1982) 369.
16 H. F. W. Taylor, Miner. Magazine J. Miner. Soc., (1876–1968) 37 (1969) 338.
17 H. C. B. Hansen and C. B. Koch, Appl. Clay Sci., 10 (1995) 5.
18 D. L. Bish and A. Livingstone, Miner. Magazine, 44 (1981) 339.
19 E. H. Nickel and R. M. Clarke, Am. Mineral., 61 (1976) 366.
20 E. Horváth, J. Kristóf, R. L. Frost, N. Heider and V. Vágvölgyi, J. Therm. Anal. Cal., 78 (2004) 687.
21 R. L. Frost, M. L. Weier and K. L. Erickson, J. Therm. Anal. Cal., 76 (2004) 1025.
22 R. L. Frost and K. L. Erickson, J. Therm. Anal. Cal., 78 (2004) 367.
23 E. Horváth, J. Kristóf, R. L. Frost, A. Rédey, V. Vágvölgyi and T. Cseh, J. Therm. Anal. Cal., 71 (2003) 707.
24 J. Kristóf, R. L. Frost, J. T. Kloprogge, E. Horváth and E. Makó, J. Therm. Anal. Cal., 69 (2002) 77.
25 F. Rey, V. Fornes and J. M. Rojo, J. Chem. Soc., Faraday Trans., 88 (1992) 2233.
26 M. Valcheva-Traykova, N. Davidova and A. Weiss, J. Mater. Sci., 28 (1993) 2157.
27 G. Lichti and J. Mulcahy, Chem. Aust., 65 (1998) 10.
28 Y. Seida and Y. Nakano, Jpn. J. Chem. Eng., 34 (2001) 906.
29 Y. Roh, S. Y. Lee, M. P. Elless and J. E. Foss, Clays Clay Miner., 48 (2000) 266.
30 Y. Seida, Y. Nakano and Y. Nakamura, Water Res., 35 (2001) 2341.
31 E. L. Crepaldi, P. C. Pavan and J. B. Valim, J. Brazilian Chem. Soc., 11 (2000) 64.
32 J. I. Di Cosimo, V. K. Diez, M. Xu, E. Iglesia and C. R. Apesteguia, J. Catal., 178 (1998) 499.
33 R. L. Frost, A. W. Musumeci, T. Bostrom, M. O. Adebajo, M. L. Weier and W. Martens, Thermochim. Acta, 429 (2005) 179.
34 T. Lopez, E. Ramos, P. Bosch, M. Asomoza and R. Gomez, Mater. Lett., 30 (1997) 279.
35 F. Malherbe and J.-P. Besse, J. Solid State Chem., 155 (2000) 332.
36 S. Miyata, Clays Clay Miner., 28 (1980) 50.
37 J. Perez-Ramirez, G. Mul and J. A. Moulijn, Vib. Spectrosc., 27 (2001) 75.
38 D. Tichit, M. H. Lhouty, A. Guida, B. H. Chiche, F. Figueras, A. Auroux, D. Bartalini and E. Garrone, J. Catal., 151 (1995) 50.
39 J. Bouzaid and R. L. Frost, J. Therm. Anal. Cal., 89 (2007) 133.
40 J. M. Bouzaid, R. L. Frost and W. N. Martens, J. Therm. Anal. Cal., 89 (2007) 511.
41 R. L. Frost, A. W. Musumeci, M. O. Adebajo and W. Martens, J. Therm. Anal. Cal., 89 (2007) 95.
42 R. L. Frost, J. M. Bouzaid, A. W. Musumeci, J. T. Kloprogge and W. N. Martens, J. Therm. Anal. Cal., 86 (2006) 437.
43 J. T. Kloprogge and R. L. Frost, J. Solid State Chem., 146 (1999) 506.
44 J. T. Kloprogge, D. Wharton, L. Hickey and R. L. Frost, Am. Mineral., 87 (2002) 623.

Received: January 9, 2008
Accepted: April 1, 2008
OnlineFirst: September 20, 2008

DOI: 10.1007/s10973-008-8992-4